Electronic Structure and Magnetism of Ordered Palladium−Manganese and Palladium−Chromium Alloys

F. Delbecq,* L. Verite, and P. Sautet

Institut de Recherches sur la Catalyse, CNRS, 2 avenue Albert Einstein, 69626 Villeurbanne Cédex, France, and Ecole Normale Supérieure de Lyon, 46 allée d'Italie, 69364 Lyon, Cédex 07, France

Received June 17, 1997. Revised Manuscript Received August 26, 1997[⊗]

In this article are presented the results of self-consistent calculations based on the density functional theory (with gradient corrections) applied on ordered binary compounds of Pd with Mn and Cr. The pure metals Pd, Mn, and Cr are also briefly considered for comparison. The results concerning the magnetic properties are in good agreement with the experimental data when they are available and hence suitable for doing predictions on the magnetic behavior of these binary systems. All four compounds studied present a "giant" moment on Mn and Cr. The results are interpreted in terms of orbital interactions with a special emphasis in the evolution of the magnetic moment with the lattice parameter. In an alloy system the metal−metal interaction is generally weaker than in a pure metal, which explains the enhanced magnetic moments.

I. Introduction

The alloys of group 10 transition metals such as Pt and Pd with more electropositive metals play an increasing role in catalysis because they show better activity and selectivity than the pure metals. The changes in the structural and electronic properties brought by alloying is a key point for a better understanding of the properties of these materials. When alloying Pd with a more electropositive metal, a charge transfer is expected and the change in the electronic population on an atom can induce important modifications in the chemisorption properties, as illustrated in the case of the $Pt_{80}Fe_{20}$ alloy.[1] The sign and amplitude of this electronic transfer is hence of indirect relevance for catalytic reactivity. These materials also show specific magnetic properties, which originate from the more or less dispersed Mn or Cr atoms in the Pd. The understanding of such electronic properties requires first-principle quantum chemical calculations. This motivated our interest in the study of binary alloys of Pd with Mn and Cr, which have been shown recently to be efficient in the CO + NO reaction[2] and butadiene hydrogenation.[3]

Well-characterized structures are known for these alloys with formula PdM or Pd_3M (M = Mn or Cr). PdMn exists in two phases depending both on the temperature and on the exact stoichiometry: the high-temperature β phase with a cubic structure (CsCl-type) and the β_1 tetragonal one (distorted CsCl structure).[4] Above a temperature of ca. 800 K, Pd_3Mn shows a disordered face-centered cubic structure (Cu_3Au-type)[5] while an ordered tetragonal structure (Al_3Zr-type) exists at lower temperature.[6] PdCr has an ordered tetragonal structure (AuCu-type).[7] Pd_3Cr is less well defined: around 25 at. % Cr, the palladium−chromium system shows a face-centered cubic (Cu_3Au-type) structure.[8]

Table 1. Mulliken Electronic Populations for fcc Pd, fcc Mn, bcc Mn, and bcc Cr

	s	p	$d_{x^2-y^2}$	d_{z^2}	d_{xy}	d_{xz}	d_{yz}
fcc Pd	0.54	0.35	1.87	1.87	1.79	1.79	1.79
fcc Mn	0.43	0.73	1.06	1.06	1.24	1.24	1.24
bcc Mn	0.45	0.75	1.04	1.04	1.24	1.24	1.24
spin-up	0.21	0.37	0.66	0.66	0.69	0.69	0.69
spin-down	0.24	0.38	0.37	0.37	0.55	0.55	0.55
Δ	−0.03	−0.01	+0.29	+0.29	+0.14	+0.14	+0.14
bcc Cr	0.34	0.74	0.81	0.81	1.10	1.10	1.10

Addition of small quantities of iron, cobalt, chromium or manganese to palladium (or platinum) creates a so-called "giant moment" with the local magnetic moment exceeding considerably the normal values found in the pure metals themselves.[9] In the ordered alloys, large moments are also found. For example, a magnetic moment of 4 μB/Mn is found in Pd_3Mn.[5,10] Some magnetic measurements made on chromium−palladium alloys show a large spin polarization on Cr from 10 at. % Cr with a maximum at 40−50 at. % Cr (4.86 μB/Cr).[11]

Some theoretical studies have been carried out on these binary compounds. Two of them deal with the antiferromagnetic order of Pd_3Mn.[12,13] In the latter, a small charge transfer from Pd to Mn is found, which seems counterintuitive considering the electropositive

[⊗] Abstract published in *Advance ACS Abstracts,* October 15, 1997.

(1) Delbecq, F.; Sautet, P. *J. Catal.* **1996**, *164*, 152.
(2) El Hamdaoui, A.; Bergeret, G.; Massardier, J.; Primet, M.; Renouprez, A. *J. Catal.* **1994**, *148*, 47.
(3) Borgna, A.; Moraweck, B.; Massardier, J.; Renouprez, A. *J. Catal.* **1991**, *128*, 99.
(4) Raub, E.; Mahler, W. *Z. Metallkde* **1954**, *45*, 430.
(5) Cable, J. W.; Wollan, E. O.; Koehler, W. C.; Child, H. R. *Phys. Rev.* **1962**, *128*, 2118.
(6) Rodic, D.; Ahlzen, P. J.; Andersson, Y.; Tellgren, R.; Bouree-Vigneron, F. *Solid State Commun.* **1991**, *78*, 767.
(7) Venkatraman, M.; Neumann, J. P. *Bull. Alloy Phase Diagrams* **1990**, *11*, 11.
(8) (a) Raub, E.; Gohle, R.; Röschel, E. *Z. Metallkde* **1967**, *58*, 567. (b) Kussmann, A.; Müller, K.; Raub, E. *Z. Metallkde* **1968**, *59*, 859. (c) Raub, E.; Mahler, W. *Z. Metallkde* **1954**, *45*, 648.
(9) Nieuwenhuys, G. J. *Adv. Phys.* **1975**, *24*, 515.
(10) Kren, E.; Kaddar, G. *Phys. Lett.* **1969**, *29*, 340.
(11) Gerstenberg, D. *Z. Metallkde* **1958**, *49*, 476.
(12) Jaswal, S. S. *Solid State Commun.* **1984**, *52*, 127.
(13) Nautiyal, T.; Auluck, S. *J. Phys.: Condens. Matter* **1989**, *1*, 2211.

S0897-4756(97)00436-5 CCC: $14.00 © 1997 American Chemical Society

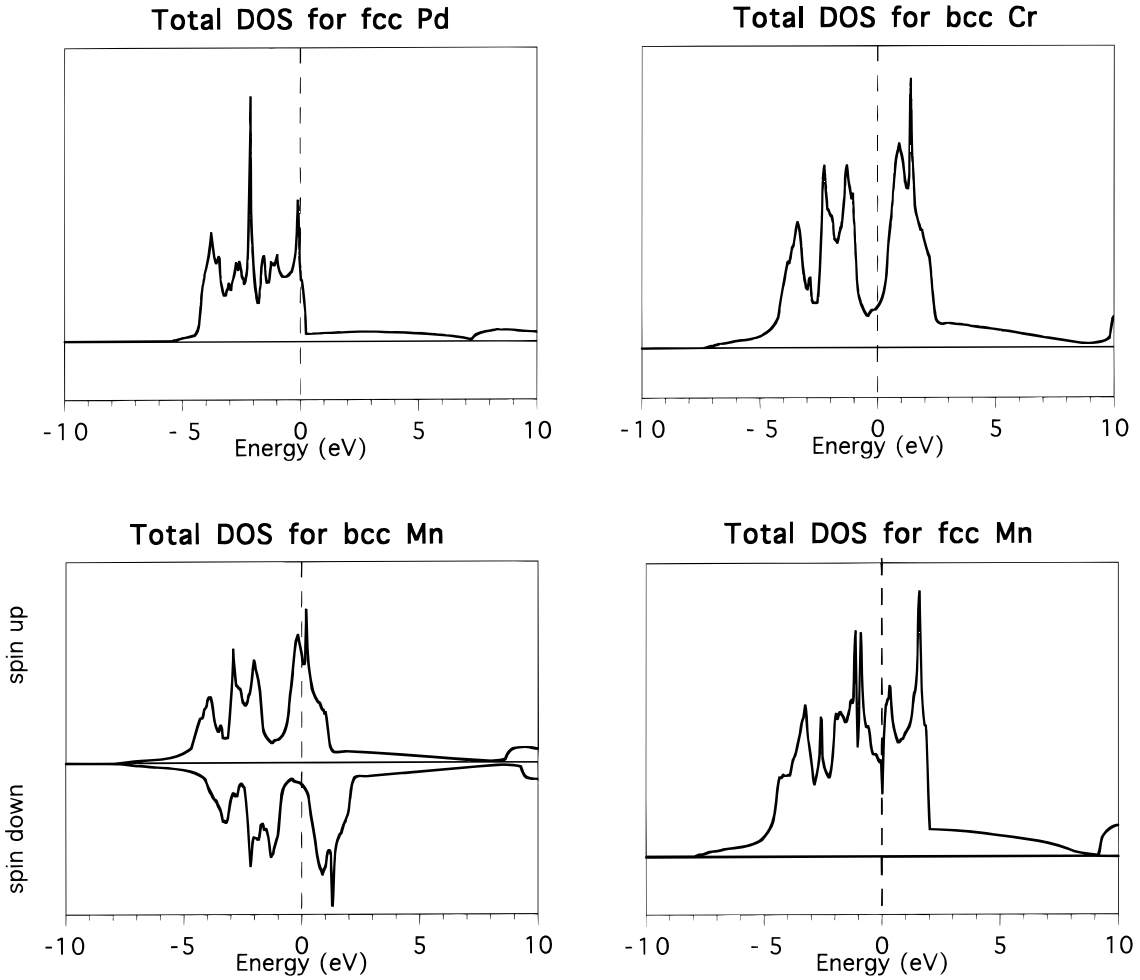

Figure 1. Total density of states (DOS) for fcc Pd, bcc and fcc Mn, and bcc Cr at their computed equilibrium geometries. For magnetic bcc Mn the DOS is projected on each spin.

character of Mn relative to Pd. Two other papers compare the electronic structure and the magnetic properties of palladium containing small amounts of Cr, Mn, Fe, Co, and Ni.[14] To our knowledge, no calculation exists for PdMn and for PdCr or Pd_3Cr alloys.

Our purpose is to describe the electronic structure of some binary PdMn and PdCr alloys of various stoichiometries, with a special emphasis on the nature of the electronic transfer between metal atoms and on the magnitude of the local atomic spin polarization, in comparison with that of pure metals. The long-range ordering of spins in ferro- or antiferromagnetic domains will not be considered. The four alloys PdMn, PdCr, Pd_3-Mn, and Pd_3Cr will be considered. The method used is a self-consistent band calculation based on the density functional theory in the Kohn−Sham approach.[15] The one-electron wave functions are developed on a basis set of atomic orbitals. These basis functions are divided into a core part (numerical orbitals) and a valence part (numerical orbitals plus Slater-type orbitals) that is of double-ζ type (see Appendix). Gradient corrections for the exchange energy (Becke 1988 or Perdew 1991) and the correlation energy (Perdew 1986 or Perdew 1991) are introduced (generalized gradient approximation, GGA). A spin-unrestricted calculation can be carried out that allows us to obtain the value of the local magnetic moment per atom in an assumed ferromagnetic state. The use of the nonlocal corrections in the SCF wave function calculations has been tested on one example (bcc Mn). It introduces no significant change in either the optimized lattice constant or in the electronic properties (orbital occupancies and magnetic moment). In each case we have first optimized the lattice parameters with a reduced number of K points and then calculated the best geometry with a larger number of K points (from 35 to 75 depending on the symmetry). The calculation of electronic populations is based on a Mulliken analysis.

II. Pure Metals, Palladium, Manganese, and Chromium

1. Palladium. The geometry optimization of fcc Pd gives a lattice constant of 4.03 Å instead of 3.89 Å as found experimentally. The 4.03 Å value corresponds to a Pd−Pd distance of 2.85 Å, slightly overestimated compared to the experimental value of 2.75 Å (+3.6%). If a LDA exchange-correlation functional is used instead of the GGA one, the correct optimum (2.75 Å) distance is obtained. However, this has to be associated with cancellation of errors since the inclusion of relativistic effects in the GGA calculation also results in a shorter bond length.[16] Other nonrelativistic LDA calculations obtained 2.79[17a] and 2.77 Å[17b] as optimum distances.

(14) (a) Mohn, P.; Schwarz, K. *J. Phys.: Condens. Matter* **1993**, *5*, 5099. (b) Oswald, A.; Zeller, R.; Dederichs, P. H. *Phys. Rev. Lett.* **1986**, *56*, 1419.

Table 2. Mulliken Electronic Populations in Pd_3Mn and PdMn

		s	p	$d_{x^2-y^2}$	d_{z^2}	d_{xy}	d_{xz}	d_{yz}	total d	total
Pd_3Mn (fcc)	Pd[a]	0.64	0.37	1.88	1.85	1.80	1.82	1.80	9.15	10.17
	spin-up	0.30	0.18	0.95	0.94	0.92	0.92	0.92	4.65	5.14
	spin-down	0.33	0.19	0.93	0.91	0.88	0.90	0.88	4.50	5.03
	Δ	−0.03	−0.01	0.02	0.03	0.04	0.02	0.04	0.15	0.11
	Mn	0.38	0.58	1.10	1.10	1.11	1.11	1.11	5.53	6.49
	spin-up	0.20	0.34	0.98	0.98	0.97	0.97	0.97	4.87	5.39
	spin-down	0.18	0.24	0.12	0.12	0.14	0.14	0.14	0.66	1.10
	Δ	0.02	0.10	0.86	0.86	0.83	0.83	0.83	4.21	4.29
PdMn (cubic)	Pd	0.73	0.45	1.83	1.83	1.82	1.82	1.82	9.12	10.32
	spin-up	0.33	0.22	0.95	0.95	0.93	0.93	0.93	4.69	5.25
	spin-down	0.40	0.23	0.88	0.88	0.89	0.89	0.89	4.43	5.07
	Δ	−0.07	−0.01	0.07	0.07	0.04	0.04	0.04	0.19	0.18
	Mn	0.49	0.63	1.97	1.07	1.14	1.14	1.14	5.56	6.68
	spin-up	0.27	0.36	0.99	0.99	0.95	0.95	0.95	4.83	5.46
	spin-down	0.22	0.27	0.08	0.08	0.19	0.19	0.19	0.73	1.22
	Δ	0.05	0.09	0.91	0.91	0.76	0.76	0.76	4.10	4.24

[a] This Pd atom lies in the front face in the *xz* plane (see Scheme 1).

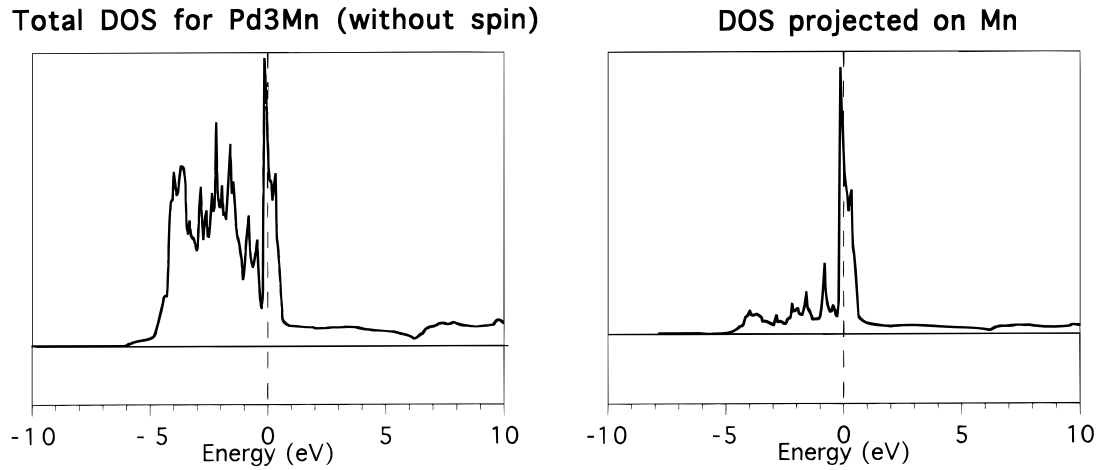

Figure 2. Total density of states (DOS) and DOS projected on Mn for non magnetic Pd_3Mn.

Scheme 1

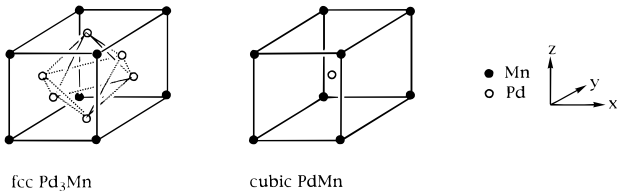

As in refs 17a,c, our calculations give a nonmagnetic state for fcc Pd at the equilibrium geometry.

The orbital occupancies calculated using the Mulliken approximation are given in Table 1. The configuration of bulk palladium in therefore $4d^{9.1}5s^{0.54}5p^{0.35}$. Such a $d^{n-1}sp^1$ configuration has also been found for the fcc 3d transition metals.[18] Table 1 shows that the d orbitals are divided in two groups which reflects the symmetry of the fcc metal (e_g and t_{2g}).

The total density of states (DOS) curve is given on Figure 1. The bandwidth is about 5 eV, which compares well with the experimental value of 5.5 eV.[19] This DOS is in good agreement with previously published calculations,[14] with the Fermi level lying at the top of the d band and with a high peak in the middle of that band.

2. Manganese. Manganese exists experimentally in four different crystal structures depending on the temperature. At low temperatures α Mn (bcc) and β Mn (c) have complex structures (58 and 20 atoms/unit cell, respectively). To obtain a reference to compare with alloys, we chose to study γ Mn (fcc) and δ Mn (bcc) that exist only at high temperatures but have simpler structures with 4 and 2 atoms/unit cell, respectively.

The geometry optimization of fcc Mn gives a lattice constant of 3.51 Å (significantly underestimated compared to the experimental value of 3.86 Å) which corresponds to a Mn−Mn distance of 2.48 Å (2.73 Å experimentally). For bcc Mn, a lattice constant of 2.85 Å is found instead of 3.08 Å experimentally, which leads to a Mn−Mn distance of 2.47 Å instead of 2.67 Å. In both cases the distances are underestimated by 8.9%. Several theoretical studies exist on the magnetic structure of γ Mn (fcc) and δ Mn (bcc).[17,20] The equilibrium lattice constant has been calculated to be 2.75[20c,d] or 2.79

(15) Te Velde, G.; Baerends, E. J. *Phys. Rev. B* **1991**, *44*, 7888; *J. Comput. Phys.* **1992**, *99*, 84.
(16) Philipsen, P., private communication.
(17) (a) Marcus, P. M.; Moruzzi, V. L. *J. Appl. Phys.* **1988**, *63*, 4045. (b) Janak, J. F. *Phys. Rev. B.* **1977**, *16*, 255. (c) Moruzzi, V. L.; Marcus, P. M. *Phys. Rev. B* **1989**, *39*, 471.
(18) Snow, E. C.; Waber, J. T. *Acta Met.* **1969**, *17*, 623.
(19) Nordlander, P.; Holloway, S.; Norskov, J. K. *Surf. Sci.* **1984**, *136*, 59.
(20) (a) Kübler, J. *J. Magn. Magn. Mater.* **1980**, *20*, 107. (b) Fry, J. L.; Zhao, Y. Z.; Brener, N. E.; Fuster, G.; Callaway, *J. Phys. Rev. B* **1987**, *36*, 868. (c) Brener, N. E.; Callaway, J.; Fuster, G.; Tripathi, G. S.; Jani, A. R. *J. Appl. Phys.* **1988**, *64*, 5601. (d) Brener, N. E.; Fuster, G.; Callaway, J.; Fry, J. L.; Zhao, Y. Z. *J. Appl. Phys.* **1988**, *63*, 4057. (e) Moruzzi, V. L.; Marcus, P. M.; Pattnaik, P. C. *Phys. Rev. B, Condensed Matter* **1988**, *37*, 8003. (f) Moruzzi, V. L.; Marcus, P. M.; Kübler, J. *Phys. Rev. B* **1989**, *39*, 6957. (g) Fry, J. L.; Zhao, Y. Z.; Pattnaik, P. C.; Moruzzi, V. L.; Papaconstantopoulos, D. A. *J. Appl. Phys.* **1988**, *63*, 4060.

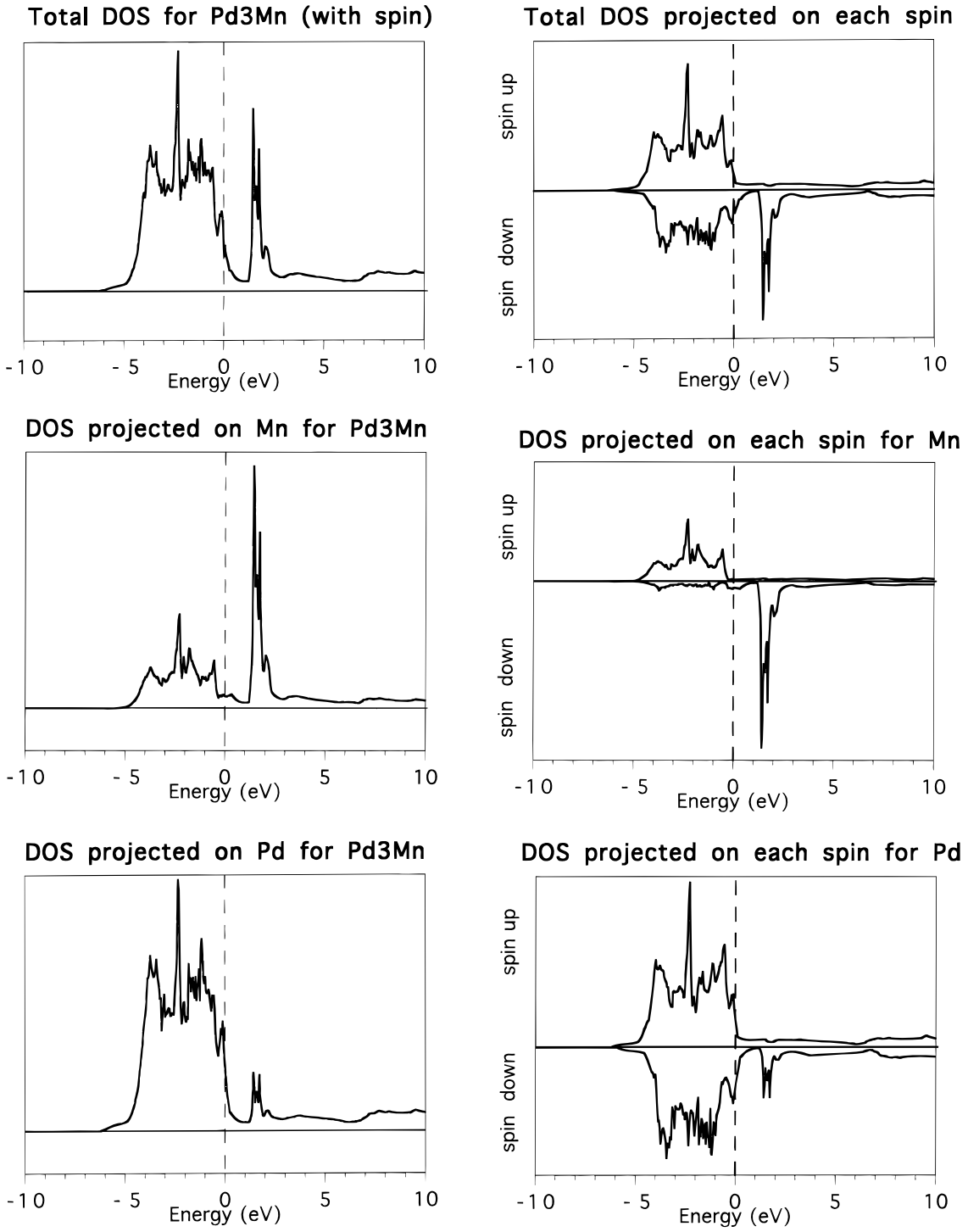

Figure 3. Total DOS and DOS projected on Mn and Pd for magnetic Pd_3Mn.

Å[17] for bcc Mn and 3.46 Å for fcc Mn,[17b] a little smaller than ours and farther from the experimental one. It has been already pointed out that the calculated equilibrium lattice constants are appreciably smaller than the experimental ones for the magnetic 3d transition metal when the spin density functional theory is used.[20a]

At our computed equilibrium lattice constants, the configuration of fcc Mn is $3d^{5.84}4s^{0.43}4p^{0.73}$ and that of bcc Mn is $3d^{5.8}4s^{0.45}4p^{0.75}$ (from Mulliken analysis, see Table 1).

An unrestricted calculation for fcc Mn at the equilibrium lattice constant surprisingly gives no magnetic moment on the metal atoms. On the contrary, such a calculation for bcc Mn gives a spin polarization (see Table 1) which results in a magnetic moment per Mn atom of 0.95 μB. It is clear from Table 1 that the magnetic moment mostly originates from the d orbitals. The closed-shell calculation gives a nonmagnetic state lying only 0.06 eV above the magnetic solution. The magnetic properties of the γ and δ forms are not clearly known from experiment. It is suggested by extrapolation that the γ fcc form should have a moment per atom near 2.4 μB and that δ bcc Mn is antiferromagnetic with a moment of about 1 μB.[21] These are however only rough estimates.

(21) Goodenough, J. B. *Phys. Rev.* **1960**, *120*, 67.

Table 3. Mullikan Electronic Populations in Pd_3Cr and PdCr

		s	p	$d_{x^2-y^2}$	d_{z^2}	d_{xy}	d_{xz}	d_{yz}	total d	total
Pd_3Cr (fcc)	Pd[a]	0.64	0.35	1.85	1.87	1.81	1.78	1.81	9.12	10.11
	spin-up	0.30	0.17	0.92	0.94	0.90	0.86	0.90	4.52	4.99
	spin-down	0.34	0.18	0.93	0.93	0.91	0.92	0.91	4.60	5.12
	Δ	−0.04	−0.01	−0.01	0.01	−0.01	−0.06	−0.01	−0.08	−0.13
	Cr	0.19	0.72	1.01	1.01	0.91	0.91	0.91	4.75	5.66
	spin-up	0.11	0.43	0.90	0.90	0.77	0.77	0.77	4.11	4.65
	spin-down	0.08	0.29	0.11	0.11	0.14	0.14	0.14	0.64	1.01
	Δ	0.03	0.14	0.79	0.79	0.63	0.63	0.63	3.47	3.64
PdCr (cubic)	Pd	0.67	0.35	1.85	1.85	1.81	1.81	1.81	9.13	10.14
	spin-up	0.30	0.17	0.97	0.97	0.90	0.90	0.90	4.64	5.10
	spin-down	0.37	0.18	0.88	0.88	0.91	0.91	0.91	4.49	5.04
	Δ	−0.07	−0.01	0.09	0.09	−0.01	−0.01	−0.01	0.15	0.07
	Cr	0.34	0.73	0.98	0.98	0.94	0.94	0.94	4.78	5.86
	spin-up	0.18	0.44	0.92	0.92	0.81	0.81	0.81	4.27	4.89
	spin-down	0.16	0.29	0.06	0.06	0.13	0.13	0.13	0.51	0.96
	Δ	0.02	0.15	0.86	0.86	0.68	0.68	0.68	3.76	3.93

[a] This Pd atom lies in the in front face in the *xz* plane (see Scheme 1).

Scheme 2

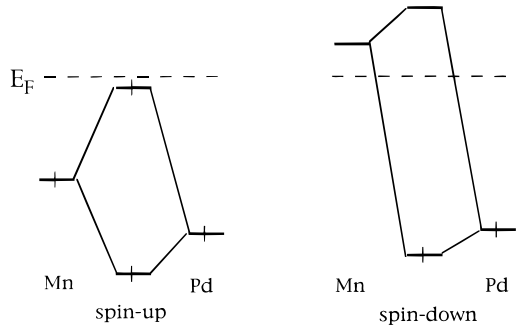

The calculated results are in good agreement with this estimate for δ bcc Mn but disagree for the γ fcc form. The magnetic moment is rather sensitive to the value of the lattice constant. Our spin-unrestricted calculations at the experimental lattice constants (3.86 Å for γ fcc Mn and 3.08 Å for δ bcc Mn) give the following results. The change is only small for bcc Mn with a magnetic moment of 1.26 μB per atom (instead of 0.95). This is in agreement with other calculations[20b,c,21] where a smooth increase of the magnetic moment with the lattice constant is found until 3.12 Å. For fcc Mn the difference is important and we find two different states at a lattice constant of 3.86 Å, one low-spin and one high-spin (1.21 and 2.09 μB, respectively), the latter being more stable by 0.07 eV. The high-spin value is in agreement with the experimental estimate.

The DOS curves for non magnetic bcc Mn and for fcc Mn at their equilibrium geometry are drawn in Figure 1.

3. Chromium. The geometry optimization of bcc chromium gives a lattice constant of 2.87 Å which leads to a Cr−Cr distance of 2.485 Å. The experimental values are 2.885 and 2.498 Å, respectively, which correspond to an error of 0.5%. Our values are in agreement with those previously calculated[20e,22a,d] where an equilibrium lattice constant of 2.78 and 2.85 Å, respectively is found. The orbital occupancies shown in Table 1 give the configuration $3d^{4.92}4s^{0.34}4p^{0.74}$ for bcc Cr. At this calculated equilibrium value, bcc Cr is found to be nonmagnetic. The corresponding DOS is given in Figure 1. In fact, Cr has been found experimentally to be antiferromagnetic with an incommensurate spin density wave.[22c] Such a complex spin state cannot be addressed by our calculations. The authors estimated the maximum Bohr magneton number to be 0.59, corresponding to an average magnetic moment of 0.46 μ_B per atom. Nevertheless our results are in agreement with previous calculations[20e,22a] where it is shown that Cr becomes magnetic for a lattice constant of 3.33 Å. We observe also an abrupt transition to a magnetic state for a lattice constant of 3.35 Å. The magnetic moment which was 0 at 3.30 Å is now 2.36 μB.

The results on the three pure metals mostly agree with the experimental data and are very close to previous calculations. Therefore we estimate that this method is trustworthy for studying the electronic properties of the alloys of these metals.

II. Binary Alloys of Palladium and Manganese

1. Pd_3Mn. As said in the Introduction, Pd_3Mn crystallizes in a disordered fcc structure above 800 K and in an ordered tetragonal one below this temperature.[6] It is based on the Cu_3Au type of order with periodic antiphase domains[10] which leads to a unit cell containing 16 atoms. We have considered here the simple fcc unit cell of Cu_3Au type, which retains the basic features such as the atom coordination.

The geometry optimization gives a lattice constant of 4.03 Å, as found for pure Pd which represents the same overestimation relative to the experimental value (3.90 Å at room temperature[6,13]). Therefore, Pd which is the larger and the more numerous species in the cell imposes its lattice structure. The electronic structure is given in Table 2. In such a crystal, a Mn atom has 12 Pd and a Pd atom has 4 Mn and 8 Pd as nearest neighbors (Scheme 1). Therefore the Mn atoms have the same symmetry as in pure fcc Mn, which is reflected by the division of the d orbitals in two groups, d_{z^2} and $d_{x^2-y^2}$ on one hand, d_{xy}, d_{xz}, and d_{yz} on the other hand. On the contrary, for the Pd atom in the *xz* plane for example, only the d_{xy} and d_{yz} orbitals have the same symmetry.

Two conclusions can be extracted from Table 2. First, from a Mulliken population analysis, Mn has lost 0.51 e^- relative to its valence number 7 and each Pd atom has received 0.17 e^- (valence number 10). Hence there is an electron transfer from Mn to Pd in agreement with

(22) (a) Moruzzi, V. L.; Marcus, P. M. *J. Appl. Phys.* **1988**, *64*, 5598. (b) Rath, J.; Callaway, J. *Phys. Rev. B*, **1973**, *8*, 5398. (c) Skriver, H. L. *J. Phys. F.: Met. Phys.* **1981**, *11*, 97. (d) Kübler, J. *J. Magn. Magn. Mater.* **1980**, *20*, 277.

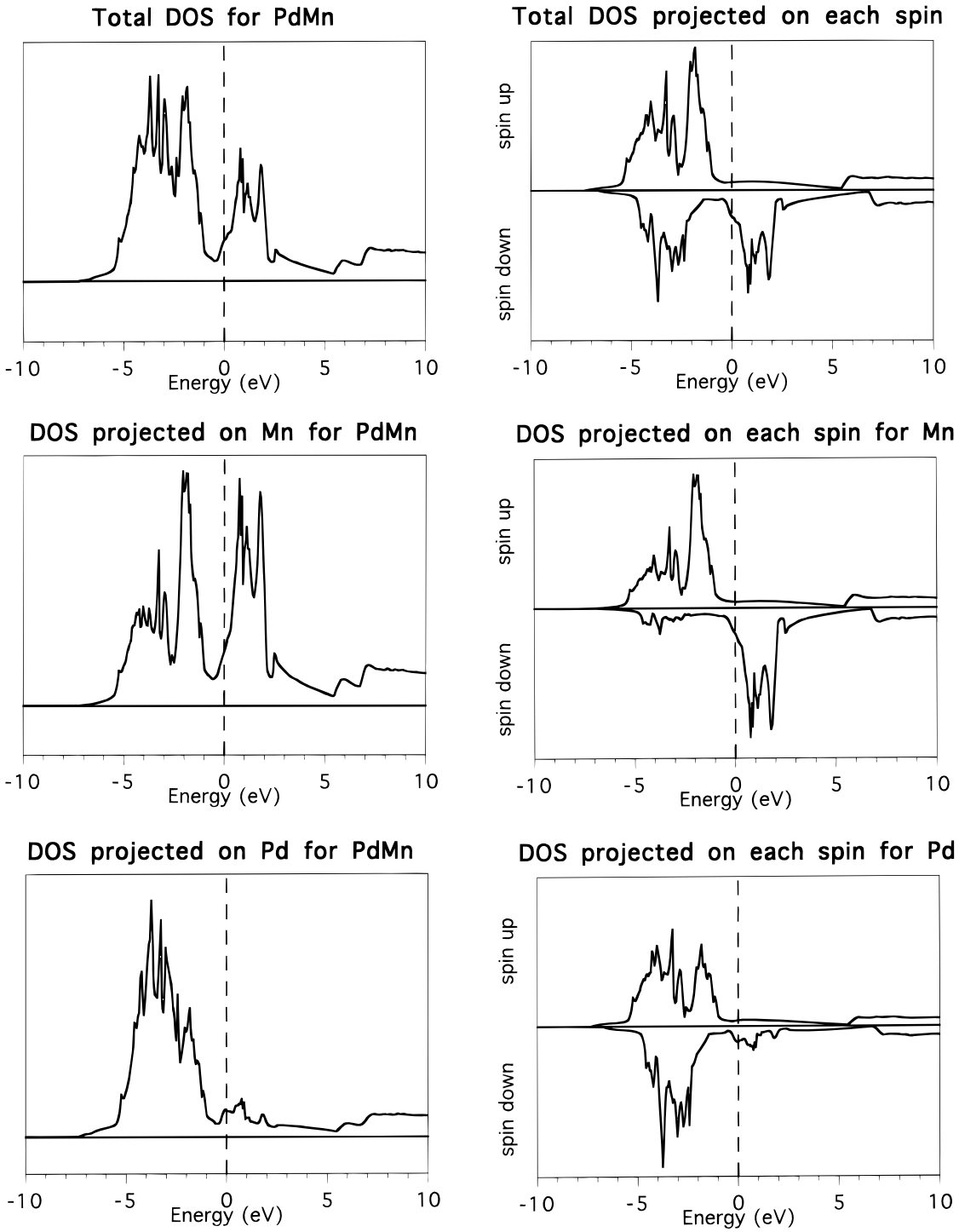

Figure 4. Total density of states (DOS) and DOS projected on Mn and Pd for magnetic PdMn (cubic).

the more electropositive character of Mn and in opposite to the result obtained in ref 13. Mulliken populations are qualitative and diffuse orbitals in the basis set can induce artifacts in the charge. However, such very diffuse orbitals that are frequent in atomic and molecular calculations are not necessary for the dense solids and are not used here. The electrons come mainly from the Mn d-orbitals (compare Tables 1 and 2) and go mainly in the Pd s orbital. Second, a magnetic moment appears both on Pd (weak: 0.11 μB) and on Mn (strong: 4.29 μB). The magnetic moment on Mn is hence much larger than that in bulk Mn and this illustrates the "giant moment effect", while a small spin polarization is induced on Pd. These values agree well with the experimental ones obtained from neutron diffraction measurements: 0.2 μB/Pd and 4.0 μB/Mn.[5,6]

The DOS curves drawn in Figure 2 correspond to a calculation for the nonmagnetic state which lies 2.3 eV above the magnetic one. This curve looks like those previously published[12,13] with a high narrow peak at the top of the band. The density of states $N(E_F)$ is large. The interactions between Mn and its Pd neighbors are less strong than in bulk fcc Mn: this is evident if the total DOS for fcc Mn (Figure 1) and the DOS projected on Mn for non magnetic Pd_3Mn (Figure 2) are compared. In the former the bandwidth is larger (ca. 6.75 vs 5 eV) and the band is equally distributed. In the magnetic case (Figure 3) the high narrow peak is pushed far above

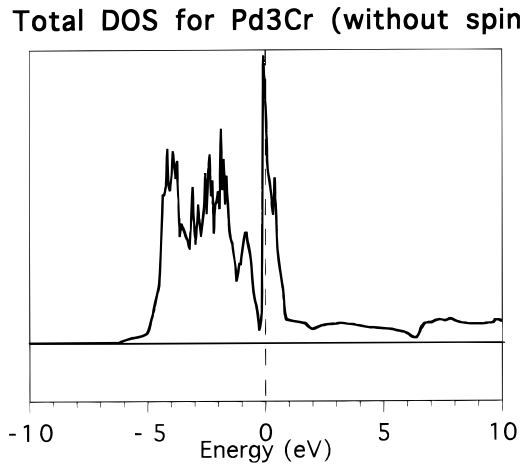

Figure 5. Total density of states (DOS) for nonmagnetic Pd_3Cr.

the Fermi level by magnetic coupling. The DOS on each spin for Mn and Pd look like those obtained for a system where Mn is considered as an impurity in palladium.[14] Indeed these systems are equivalent for Mn if only first-neighbor interactions are considered. In free Mn atom the spin-up d-band is totally full and the spin-down d-band totally empty. For Pd atoms, both bands are full.

The interactions between spin-up and between spin-down orbitals of Pd and Mn are depicted in Scheme 2, where only one spin−orbital of each type is considered. The interactions between the spin-up orbitals of Mn and Pd being weaker than between two Mn atoms give bands which remain almost entirely under the Fermi level as can be seen in Figure 3 and the spin-up d-bands are almost full ($4.87e^-$ and $4.65e^-$ for Mn and Pd, respectively). The spin-down orbitals of Mn are pushed toward higher energies (compare Figures 2 and 3) by interaction with the spin-down orbitals of Pd. This weak interaction leads to a small contribution of the occupied spin-down orbitals of Pd to vacant levels and of the vacant spin-down orbitals of Mn to occupied levels. Hence the spin-down electronic population of Pd is reduced and only a small spin-down occupation appears on Mn. These occupations are $4.5e^-$ and $0.66e^-$, respectively. This analysis explains why Mn has a larger magnetic moment in Pd_3Mn than in pure metal and why a small moment appears on Pd.

2. PdMn. As recalled earlier, PdMn exists in a high-temperature cubic structure of CsCl-type with $a = 3.174$ Å. It can also exist as tetragonal (distorted CsCl) structure with a c/a ratio depending on the exact stoichiometry of Mn in the alloy.[4] The optimization of the cubic structure gives a lattice constant of 3.179 Å, close to the experimental value with a Pd−Mn distance of 2.753 Å. The optimization of the tetragonal structure, first at constant c/a, then by varying c/a until 1, leads to a smaller c/a ratio than the experimental one (1.124 instead of 1.245 for 50% at. Mn) with $a = 3.048$ Å and $c = 3.455$ Å. The tetragonal structure is more stable than the cubic one by 0.16 eV, and such a relative stability is expected from the experimental phase diagram.

For symmetry reasons, the cubic structure is easier to study and the interpretations will be simpler. Moreover, the two structures give very similar results in what concerns the electron transfer between Mn and Pd and the magnetic moments. Hence we will focus on the cubic structure in the following. The electronic structure is given in Table 2. Each atom of one metal has 8 nearest neighbors of the other metal (Scheme 1) and hence the orbitals are divided in two groups both for Mn and Pd, d_{z^2} and $d_{x^2-y^2}$ on one hand (e_g), d_{xy}, d_{xz}, and d_{yz} on the other hand (t_{2g}) as in bcc Mn. As in Pd_3Mn there is an electron transfer from Mn to Pd (0.32 e^-) and a magnetic moment both on Mn (4.24 μB) and on Pd (0.18 μB). The electron transfer is again mainly from 3d Mn orbitals to the 5s Pd orbital. It is smaller than in Pd_3Mn because the electronic population transferred from each Mn is concentrated on one Pd atom instead of being distributed on three Pd atoms. The variation of the magnetic moment is small compared to Pd_3Mn despite the fact that the concentration in Mn varies from 0.25 to 0.5.

In PdMn, a Mn atom is less isolated than in Pd_3Mn. Indeed, even if all the neighbor atoms are still Pd, it has only 8 Pd as neighbors instead of 12, and the other Mn atoms are not so far away (3.18 Å instead of 4.03 Å) so that the interactions between Mn atoms are not negligible. Each interaction between a Mn and a Pd atoms is also stronger because the Pd−Mn distance is shorter (2.75 vs 2.85 Å). The result is that the band projected on Mn is not as narrow as it was in Pd_3Mn (compare Figures 3 and 4), especially the part above the Fermi level, which was almost a simple peak in Pd_3Mn and is here relatively broad. On the contrary, a Pd atom has 8 Mn as first neighbors instead of 4 Mn and 8 Pd in Pd_3Mn. Hence the global interaction of a Pd atom with its first neighbors is smaller despite the shorter distance and the d-band projected on Pd is narrower than for Pd_3Mn. For both Pd and Mn, one observes that the occupied part of the d-band is farther from E_F relative to Pd_3Mn owing to an increase of the Fermi level energy (higher concentration in Mn). The interactions between the spin-up and between the spin-down orbitals of Mn and Pd are of the same kind as before (see Scheme 2). Since a Pd atom is more isolated in PdMn than in Pd_3Mn and since its global interaction with its neighbors is smaller, the antibonding interactions of the spin−orbitals of Pd and Mn are less destabilized (see Scheme 2). Therefore the spin-up occupation of the Pd d orbitals is slightly increased compared to Pd_3Mn ($4.69e^-$ versus $4.65e^-$) and, on the contrary, its d spin-down occupation is reduced ($4.43e^-$ versus $4.50e^-$). This results in a slightly larger magnetic moment on Pd (0.18 vs 0.11 μB).

Concerning Mn atoms, let us consider for comparison a Pd_3Mn structure with the same Pd−Mn distance as in PdMn (2.75 instead of 2.85 Å), for which the Mn magnetic moment is 4.15 instead of 4.29 μB. The interactions of a Mn atom with its first Pd neighbors are less numerous in PdMn than in Pd_3Mn (8 instead of 12 neighbors). This results in a weaker total interaction and hence in a larger moment (4.24 vs 4.15 μB). The fact that μ is larger for Pd_3Mn at the equilibrium geometry is due to the larger Pd−Mn distance.

IV. Binary Alloys of Palladium and Chromium

1. Pd_3Cr. The Pd−Cr system is not as well-known as the PdMn one. Nevertheless, a study of the Pd−Cr solid solutions by varying the percentage of Cr shows that around 25 at. % Cr the structure is fcc (Cu_3Au type)

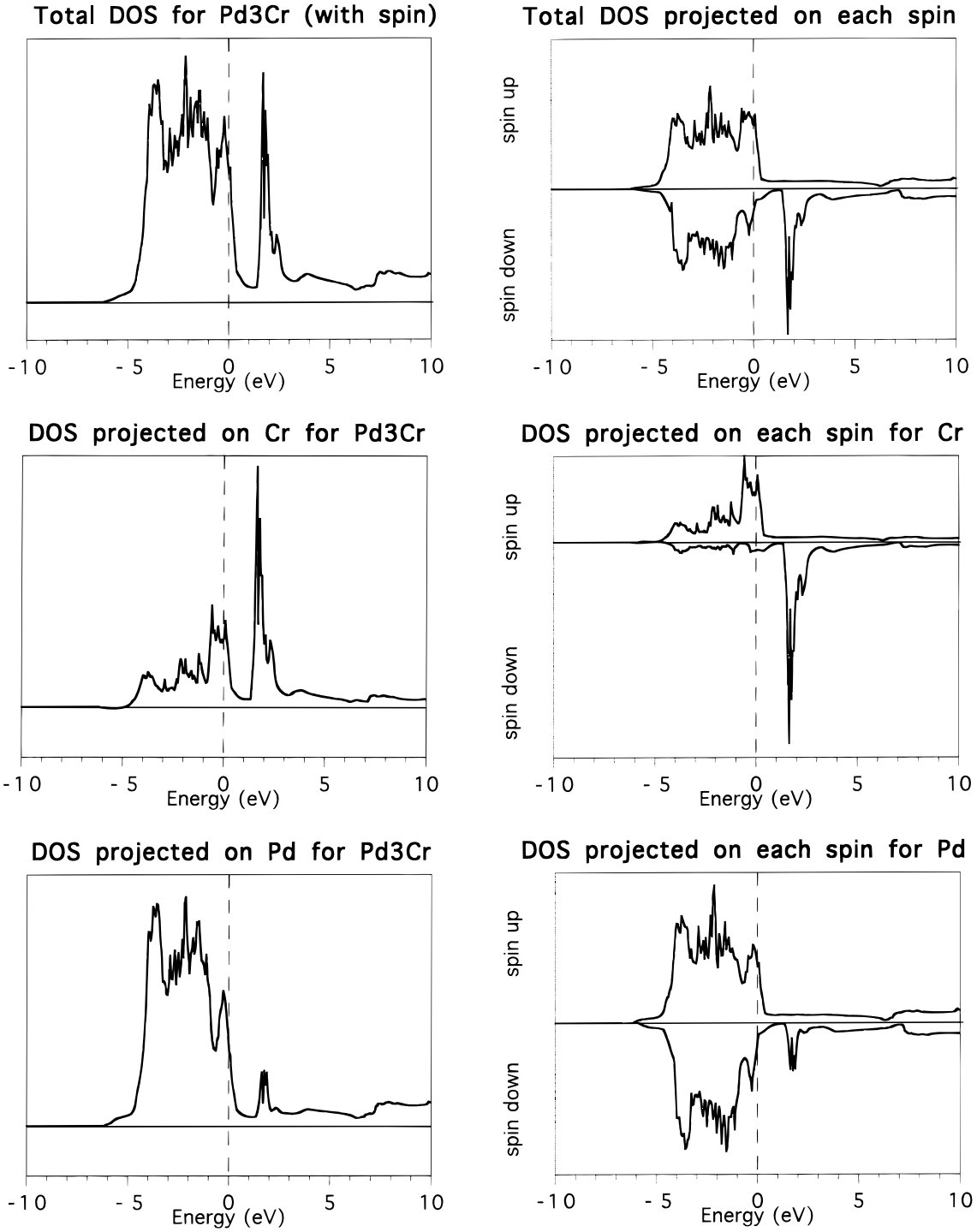

Figure 6. Total density of states (DOS) and DOS projected on Cr and Pd for magnetic Pd_3Cr.

with a lattice parameter of 3.865 Å[8c] or 3.874 Å.[7] After geometry optimization, our calculations give a lattice constant of 4.03 Å as for Pd_3Mn and pure Pd with a similar overestimation compared to the experimental values.

The electronic occupations, as obtained from a Mulliken analysis, are given in Table 3. One observes an electron transfer of $0.34e^-$ from the Cr atom to the three Pd atoms in agreement with the electronegativity difference of the two metals. As for Pd_3Mn, the main transfer occurs between the d-orbitals of Cr and the s-orbital of Pd, nevertheless the s orbital of Cr plays a nonnegligible role. A strong magnetic moment exists on Cr (3.64 μB). The palladium atoms also have a small magnetic moment but the spin polarization is opposite to that in Pd_3Mn (−0.11 μB). The same spin polarization is found for Pd atoms in calculations where Cr is only an impurity in the Pd lattice.[14] In these works, the magnetic moment on Cr has been calculated to be 2.86 and 3.14 μB, respectively.

The examination of the DOS curves for Pd_3Cr (Figures 5 and 6) shows that the same explanation as for Pd_3Mn is valid in what concerns the magnetic moment on Cr atoms. For the opposite polarization of Pd atoms, the following explanation is proposed. The element Cr has more expanded d-orbitals than Mn, and thus the overlaps with Pd orbitals are better for Cr than for Mn. This leads to a better interaction between Pd and Cr

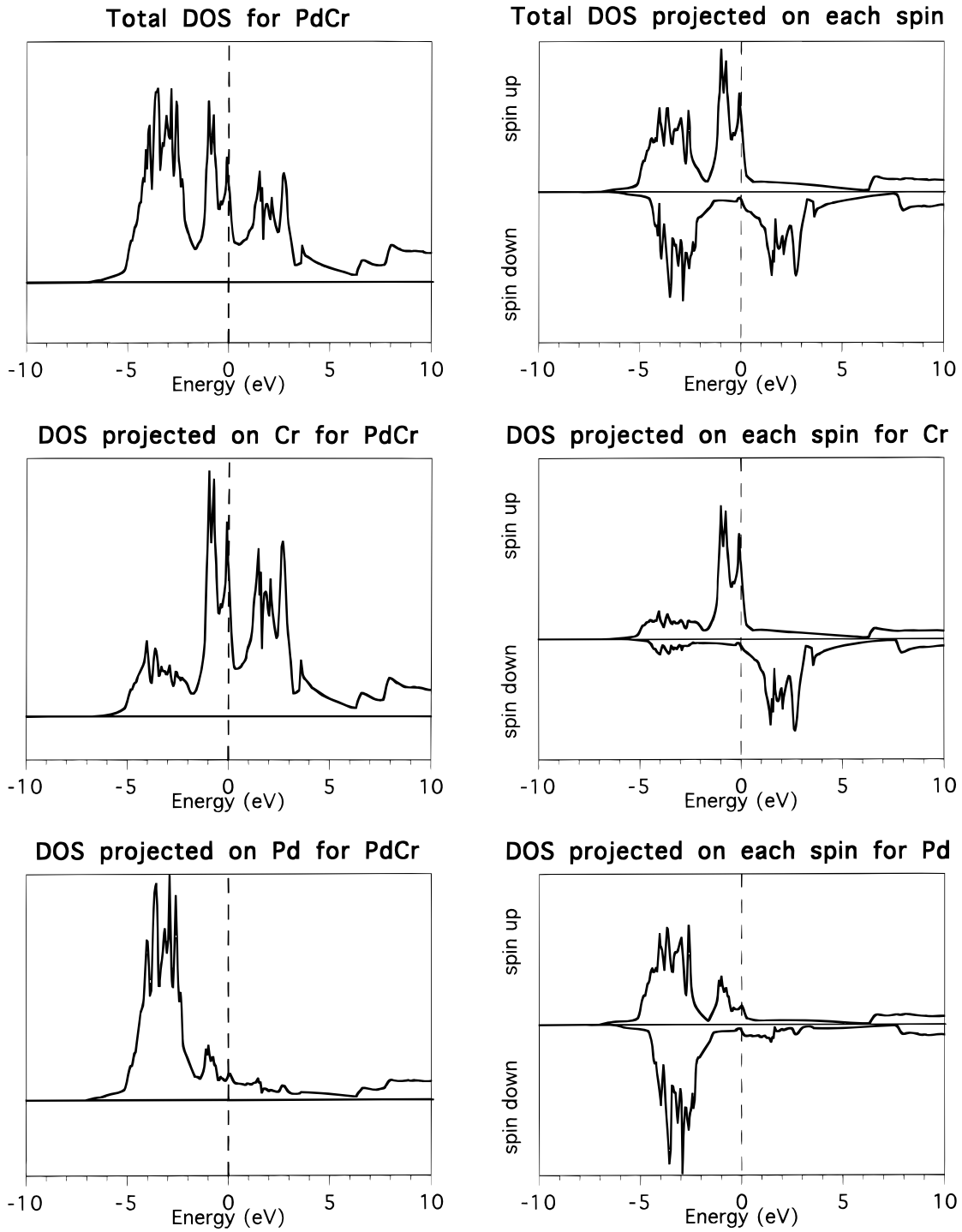

Figure 7. Total density of states (DOS) and DOS projected on Cr and Pd for magnetic PdCr.

atoms resulting in a larger d band in the DOS for Pd_3Cr than for Pd_3Mn (compare Figures 2 and 5). The difference in d bandwidth is about 0.45 eV. If we consider now Scheme 2, the better interaction between the spin-up orbitals of Pd and Cr has the consequence that the antibonding part of the band is partly pushed above the Fermi level instead of being entirely below this level as it was in the case of Pd_3Mn (compare the spin resolved DOS projected on Pd in Figures 3 and 6). Hence the spin-up d-orbitals of Pd atom are less occupied in Pd_3Cr relative to Pd_3Mn ($4.52e^-$ versus $4.65e^-$ from Table 3). In what concerns the spin-down orbitals, the better interaction of the occupied spin-down d-orbitals of Pd with the empty spin-down d-orbitals of Cr lowers the former more than in the case of Pd_3Mn, and hence the major part of the spin-down d-band of Pd is below E_F (compare Figures 3 and 6). Therefore in the case of Pd_3Cr, the spin-down occupation of Pd d orbitals is larger than in Pd_3Mn ($4.6e^-$ versus $4.5e^-$ from Table 3). As a result for the d-orbitals of Pd, the spin-down occupation becomes larger than the spin-up one, which explains the inverse polarization of Pd in Pd_3Cr if one neglects the s- and p-orbitals. Of course the d-orbital, which is the most responsible for the spin polarization, is d_{xz} (-0.06) since that is the one which has the better interaction with the Cr atoms in a fcc-type structure (see Scheme 1). It represents half of the total Pd spin polarization (Table 3).

2. PdCr. PdCr has a well-defined tetragonal structure of AuCu-type, which can be described by a body-

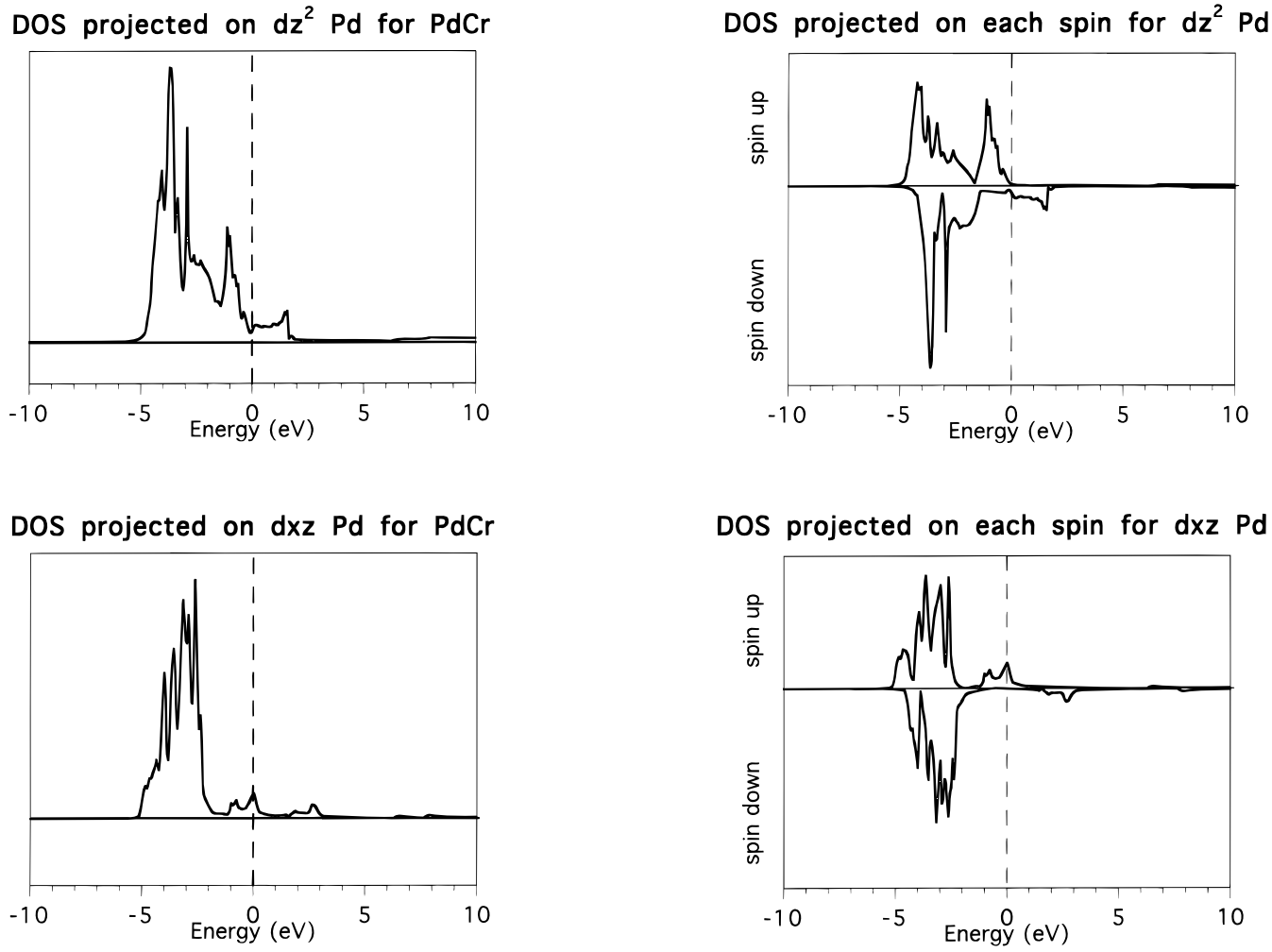

Figure 8. DOS projected on d_{z^2} and d_{xy} orbitals of Pd for magnetic PdCr.

centered tetragonal (bct) unit cell with $a = 2.74$ Å and $c = 3.80$ Å.[7] The c/a ratio of 1.39 is close to the limit value of $c/a = \sqrt{2}(1.41)$ which gives a fcc lattice with parameter c. Since for PdMn we have studied a cubic structure of CsCl type, we have also envisaged such a structure for PdCr. The geometry optimization of cubic PdCr gives a lattice constant of 3.19 Å which corresponds to a PdCr distance of 2.76 Å. Then, the geometry optimization of the tetragonal structure at constant c/a (1.39) gives $a = 2.83$ Å and $c = 3.92$ Å, which represents an overestimation of 3.2%. By varying c/a from 1.39 to 1, which corresponds to the cubic value, one obtains the best geometry for $a = 3.0$ Å and $c = 3.59$ Å with $c/a = 1.19$. This structure is 0.3 eV more stable than the previous one ($c/a = 1.39$) and 0.1 eV more stable than the cubic one. As in the case of PdMn, the optimized c/a value is underestimated. However the trend of a larger c/a for PdCr than for PdMn is correctly reproduced.

In both the tetragonal and the cubic structures, there is an electron transfer of $0.14e^-$ from Cr to Pd, smaller than for Pd_3Cr (as in PdMn compared to Pd_3Mn). The magnetic moment on Cr is large (3.85 μB for tetragonal and 3.93 μB for cubic). To our knowledge, only one experimental determination exists for the magnetic moment in PdCr:[11] the spin quantum number found is 2.08, corresponding to a magnetic moment of 4.16 μB. The spin polarization on Pd is small (0.03 μB for tetragonal and 0.07 μB for cubic) but positive, contrary to what happens in Pd_3Cr. As for PdMn, the difference between the tetragonal and cubic structures is small, and we will concentrate on the cubic one which is simpler for symmetry reasons. Its electronic structure is given in Table 3.

The same differences exist between the DOS curves of PdCr and Pd_3Cr as between those of PdMn and Pd_3Mn (compare Figures 7 and 6) and for the same reason. The total d-band is broader for PdCr and especially the empty part of the DOS projected on Cr, which was very narrow in Pd_3Cr. On the contrary, the Pd-projected band gives a much narrower band. However, the differences between the two alloy stoichiometries are amplified compared to the Pd−Mn alloys because of the greater extension of the Cr orbitals which implies stronger interactions between Cr and Pd.

The Cr magnetic moment is much larger than in Pd_3Cr (3.93 vs 3.64 μB) and even larger if one considers a Pd_3Cr structure with the same Pd−Cr distance (3.2 μB). The explanations are the same as previously for the Pd−Mn alloys: the interactions between Cr and Pd are less numerous in PdCr relative to Pd_3Cr, but the effects are enhanced by the strength of the Pd−Cr interaction compared to the Pd−Mn one.

The different behavior of the e_g (d_{z^2} and $d_{x^2-y^2}$) and t_{2g} (d_{xy}, d_{xz}, d_{yz}) sets of Pd orbitals is shown in Figure 8 for d_{z^2} and d_{xz}. The t_{2g} set is well directed to interact with the Cr atoms of the corners and a fraction of the spin-up orbitals is therefore pushed above the Fermi

level. This lowers the population of the spin-up t_{2g} set, which finally results in a negative spin polarization. On the contrary, the e_g set interacts less strongly with the Cr atoms and all the spin-up orbitals remain below the Fermi level, resulting in a positive spin polarization.

V. Conclusion

The results obtained in this work on alloys are in good agreement with the experimental data. The method used, based on first principle LCAO periodic calculations using the DFT theory at the nonlocal level, is suitable for such systems and can be successfully compared with other methods based on the APW approach for studying ferromagnetic states. An advantage of the method is that it allows an easy analysis of the interactions between atomic orbitals. Hence we can discuss the qualitative features of the electronic structure and the appearance of the magnetic moment with an atomic orbital viewpoint.

Some general results are obtained:

(i) The alloying of Pd with more electropositive elements such as Mn or Cr results in an electron transfer from these metals to Pd. The transfer is smaller for the Pd−Cr alloys reflecting that Cr is slightly less electropositive than Mn.

(ii) This alloying induces a magnetic moment, very strong on Mn or Cr compared to pure metal and small on Pd, which is nonmagnetic when it is not alloyed. Hence there is an important spin polarization due to the alloying. Our calculations are thus in agreement with the "giant" moment found experimentally in such alloys.

(iii) The Mn magnetic moment varies little when the concentration in Mn changes from 0.5 to 0.25 (4.24 to 4.29 μB). Similar calculated values are obtained for systems where Mn is an impunity in Pd (31 Pd atoms around 1 Mn atom)[14] since the values obtained are 3.96[14a] and 4.13 μB.[14b] The same observation has been made in the study of the series Co_3Pt, CoPt, $CoPt_3$.[23]

The variation of the Cr magnetic moment with the concentration of Cr is larger for the Pd−Cr alloys (3.93 to 3.64 μB) and such a difference also exists for the system where Cr is an impurity in Pd (2.86[14a] and 3.14 μB[14b]). An interesting result for the Pd−Cr alloys is that the Pd moment is opposite to that of Cr when the concentration of Cr is not too large (Pd_3Cr and Pd lattice with Cr impurities). All these different properties of the Pd−Cr alloys compared to the Pd−Mn alloys are explained and related to the stronger Pd−Cr interaction.

The key for obtaining such a large magnetic moment is that the potentially magnetic atom (here Mn $3d^5 4s^2$ or Cr $3d^5 4s^1$) is sufficiently isolated in the middle of atoms of other types (with different energy position and orbital expansion). The interactions with the environment are then minimal, compared to the degenerate interaction in the case of pure metal, and hence the atom is as close as possible to its atomic state.

Appendix

Slater exponents used in this work:

Pd 4s: 3.85; 4p: 3.15; 4d: 1.5; 5s: 1.85; 5p: 1.85 (simple ζ)

Mn 3s: 3.5; 3p: 3.0; 3d: 1.2; 4s: 2.0; 4p: 1.5 (simple ζ)

Cr 3s: 3.25, 3p: 2.85; 3d: 1.7; 4s: 1.9; 4p: 1.3 (simple ζ)

Acknowledgment. The authors thank the Institut du Développement et des Ressources en Informatique Scientifique, IDRIS (CNRS Orsay) for the attribution of CPU time (Project No. 950613).

CM970436M

(23) Kootte, A.; Haas, C.; de Groot, R. A. *J. Phys.: Condens. Matter* **1991**, *3*, 1131.